

# AirLoop: Lifelong Loop Closure Detection

Dasong Gao, Chen Wang<sup>†</sup>, and Sebastian Scherer

**Abstract**—Loop closure detection is an important building block that ensures the accuracy and robustness of simultaneous localization and mapping (SLAM) systems. Due to their generalization ability, CNN-based approaches have received increasing attention. Although they normally benefit from training on datasets that are diverse and reflective of the environments, new environments often emerge after the model is deployed. It is therefore desirable to incorporate the data newly collected during operation for incremental learning. Nevertheless, simply finetuning the model on new data is infeasible since it may cause the model’s performance on previously learned data to degrade over time, which is also known as the problem of catastrophic forgetting. In this paper, we present AirLoop, a method that leverages techniques from lifelong learning to minimize forgetting when training loop closure detection models incrementally. We experimentally demonstrate the effectiveness of AirLoop on TartanAir, Nordland, and RobotCar datasets. To the best of our knowledge, AirLoop is one of the first works to achieve lifelong learning of deep loop closure detectors.

## I. INTRODUCTION

Loop closure detection (LCD) is an important building block of modern simultaneous localization and mapping (SLAM) systems. Despite tremendous efforts to improving its accuracy and robustness, visual SLAM is still vulnerable to cumulative errors [1]. LCD helps combat this problem by identifying the revisited scenes and places, which allows the robot to reduce localization and mapping drift introduced by sensor measurement errors and scene abnormalities such as occlusion and motion blur [2].

Traditional LCD algorithms leverage handcrafted features like HoG [3], SIFT [4], and SURF [5] to generate visual words and build the bag-of-words (BoW) model [6]. Such methods are, however, vulnerable to environmental changes including illumination, weather, and viewpoint, which can greatly alter the local texture [1]. In contrast, CNN-based approaches have received increasing attention due to their higher precision, robustness, and generalization ability [7].

However, CNN-based approaches are data-driven. To maintain the aforementioned advantages, it requires training data to be diverse and reflective of the working environment [8]. This cannot be always satisfied since the new environments we encounter after model deployment may look different from the training set [9], [10]. In this sense, we often expect that a model can learn from new data incrementally.

Nevertheless, continual learning in different environments is difficult. Unlike traditional methods such as BoW, which

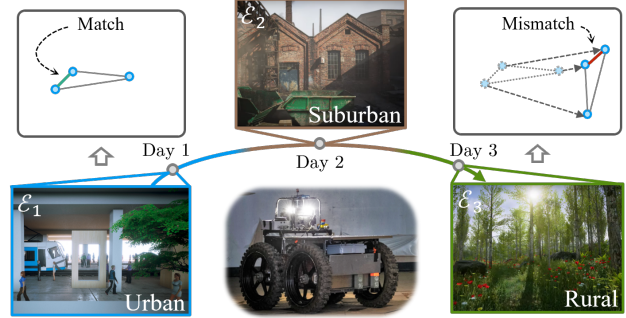


Fig. 1: A robot may encounter a series of new environments ( $\mathcal{E}_1, \mathcal{E}_2, \dots$ ) after deployment, in which case the robot may benefit from incremental learning in new environments. However, directly retraining on newly collected data deforms previously learned descriptors, which may cause similar descriptors to separate and distinct descriptors to come close. This will lead to ambiguity and eventually mismatches that are harmful for loop closure detection. In this paper, we resort to lifelong learning to tackle such issues.

learns new scene representation by simply expanding the visual vocabulary with new data [10], deep LCD models typically need to adjust all parameters jointly to adapt to new environments. This poses a dilemma: On the one hand, if we only retrain on the data increments, fitting to the new data almost inevitably alters the parameters and, subsequently, the descriptor space learned from the old data, leading to performance degradation over time, as shown in Fig. 1. This phenomenon is referred to as catastrophic forgetting [11], [12]. On the other hand, if all previously observed data is retained to perform joint training after observing each new environment, the storage cost will grow linearly as the model learns from one environment to the next. This is prohibitive on resource-constrained devices such as a drone’s onboard computer. The question is therefore: Can we train a deep LCD model from a video stream without suffering from forgetting?

In this work, we address the two problems of incrementally learning a deep LCD model by proposing AirLoop, a lightweight lifelong learning method for loop closure detection. Specifically, we adapt two lifelong learning techniques that have been used for image classification: memory aware synapses (MAS) [13] and knowledge distillation (KD) for lifelong embedding learning [14]. We also propose a similarity-aware memory buffer that caches samples from a small moving window on the data stream. This allows us to train the LCD model in a series of environments sequentially without suffering from serious catastrophic forgetting while

<sup>†</sup>Corresponding Author. This work was partially sponsored by ONR grant #N0014-19-1-2266 and ARL DCIST CRA award W911NF-17-2-0181.

The authors are with the Robotics Institute, School of Computer Science, Carnegie Mellon University, Pittsburgh, PA 15213, USA. E-mail: dasongg@andrew.cmu.edu; chenwang@dr.com; basti@andrew.cmu.edu

Source Code: <https://github.com/wang-chen/AirLoop>.

only requiring constant memory and computation. To the best of our knowledge, AirLoop is one of the first work to study LCD in the lifelong learning context.

In summary, our contribution includes:

- For the first time, we formulate the lifelong loop closure detection problem to study possible ways to continually improve the robustness of a visual SLAM system.
- We introduce a relational variant of MAS for embedding learning in the context of lifelong loop closure detection.
- We propose a similarity-aware memory buffer that allows efficient triplet sampling from streaming data.
- Through extensive experiments on three datasets, we demonstrate the advantage of our method in alleviating catastrophic forgetting and encouraging generalization.

## II. RELATED WORK

### A. Lifelong Learning

Lifelong learning, also known as continual, incremental, or sequential learning, aims at incrementally building up knowledge from an infinite stream of data [15]. The most challenging aspect of lifelong learning is the catastrophic forgetting problem, where fitting to newly arrived data or tasks deteriorates the model’s performance on previously observed ones [11], [12]. Recent works on overcoming catastrophic forgetting roughly fall into three families: rehearsal, parameter isolation, and parameter regularization [15].

Rehearsal methods such as iCaRL [16], GEM [17], ER [18], and SER [19] selectively store a small subset of observed data as exemplars and replay them when new data is introduced. Some recent methods [20], [21] replay synthetic samples from the generative adversarial networks (GANs).

Parameter isolation methods alleviate the catastrophic forgetting by dedicating model parameters to specific tasks [15]. Additive approaches such as LwF [22] and EBL [23] introduce new classification heads for each incoming set of classes. In contrast, subtractive approaches like PackNet [24] and Piggyback [25] incrementally freeze the trained part of the network to achieve theoretically zero forgetting.

Regularization methods take effect by protecting parameters that are important for previously learned tasks. To define importance, EWC [26] uses the estimated diagonal of the model’s Fisher information matrix through back-propagation. Similarly, SI [27] calculates the per-parameter contribution to loss decrease during the training of previous tasks. Riemannian Walk [28] combines the path integral from SI and an online version of EWC. MAS [13] defines the importance as the model’s sensitivity to the parameters, which is the magnitude of the gradient. To retain the pairwise embedding distance of previously learned relations, [29] imposes a maximum mean discrepancy (MMD)-based distillation loss. [30] incorporates all previous teacher’s knowledge by estimating their outputs with a random perturbation process. To tackle lifelong learning in graph networks, [31] converted the node classification to graph classification via feature interaction.

Our method includes a variant of MAS (RMAS) optimized for contrastive learning, where we measure the sensitivity of

descriptors’ pairwise similarities instead of the exact values. In the experiment section, we show that our relational MAS gives a better performance than the original MAS. Our work is also related to [30] as we also employ a relational knowledge distillation (RKD) loss to further improve its efficacy. By combining both parameter regularization and knowledge distillation, our method leads to better preservation of previously learned knowledge as shown by the experiments.

### B. Loop Closure Detection

Loop closure detection aims at identifying images that capture the same place of the 3D space from a large image database [7]. To achieve this, traditional LCD methods like Galvez-López and Tardós [32], FAB-MAP [33], and FAB-MAP 3D [34] build a BoW model with visual words generated from handcrafted features offline. More recently, IBuLD [35] proposes to dynamically build an environment-specific vocabulary, which is improved in iBoW-LCD [10] by introducing a tree indexing structure and a RANSAC-based refine step to achieve higher efficiency and accuracy.

In deep learning-based methods, a CNN is trained to generate vector-valued global descriptors for each image, and matching images are retrieved based on descriptor similarities. Many of such networks employ an extractor-aggregator architecture. Specifically, given an input image, a feature extractor based on backbones such as VGG [36], ResNet [37], or Inception [38] generates a dense feature map, which is then aggregated into a single vector with methods like NetVLAD [39], R-MAC [40], or GeM [41].

Despite having similar goals, our setting differs from the majority of deep LCD in that while regular LCD training allows access to the *full* dataset throughout the training process, data samples in our setting become available only *gradually* in a *sequential order*. It is, therefore, necessary to take measures against the catastrophic forgetting issue.

We also note that there is one line of work known as long-term LCD, which sounds similar to but is different from lifelong LCD. Long-term LCD aims at improving the robustness of loop closure detection against environmental changes such as season, weather, and illumination by learning a unified representation of the environment [7], [42]. However, to achieve this consistency, long-term LCD models are allowed access to the entire dataset during training [43], [44], [45], which is not possible under the lifelong setting. Further, many of the long-term LCD methods employ mechanisms for focusing on elements of the scene that are more stable under environmental changes [46], [47], [43], [44], [45], [48]. However, none of them studied the catastrophic forgetting during knowledge accumulation. This makes our work the first to consider LCD in the lifelong learning context.

## III. PROBLEM FORMULATION

For completeness, we start with the regular loop closure detection. Let environment  $\mathcal{E} = (\mathcal{I}, l)$ , where  $\mathcal{I}$  is the set of all images captured from the environment and  $l : \mathcal{I} \times \mathcal{I} \mapsto \{0, 1\}$  is the ground truth indicator that outputs 1 for image pairs forming a loop. Given a query image  $I \in \mathcal{I}$  and database

images  $\mathbf{D} \subset \mathcal{I}$ , the regular loop closure detection  $C(I, \mathbf{D})$  aims at finding the images in  $\mathbf{D}$  that form a loop with  $I$ :

$$C(I, \mathbf{D}) = \{I' \in \mathbf{D} : l(I', I) = 1\}. \quad (1)$$

When training on a dataset comprised of  $T$  environments,  $\{\mathcal{E}^{(i)}\}_{i=1}^T$ , where  $\mathcal{E}^{(t)} = (\mathcal{I}^{(t)}, l^{(t)})$ , the model is allowed to access the full set of images  $\bigcup_{t=1}^T \mathcal{I}^{(t)}$  at every training step. After training, the model is asked to predict loop closure in an observed or unobserved environment:

$$C^{(t)}(I, \mathbf{D}) = \{I' \in \mathbf{D} : l^{(t)}(I', I) = 1\}, \quad (2)$$

where  $I \in \mathcal{I}^{(t)}$ ,  $\mathbf{D} \subset \mathcal{I}^{(t)}$ .

In lifelong loop closure detection, one is allowed to access the environments and the frames in the environments *only in sequential order*, and each data sample is available *only once*. In other words, the model learns from the labeled video stream one frame at a time:

$$(I_1^{(1)}, l^{(1)}), \dots, (I_{N_1}^{(1)}, l^{(1)}), (I_1^{(2)}, l^{(2)}), \dots, \quad (3)$$

where all  $N_i$  images from environment  $i$  are observed before switching to the next. As mentioned earlier, this is due to the limited computational and storage resources of a robot's onboard computer, which forbids joint training using the full set of historical data. Such a setting is very challenging in that: 1) Since samples are observed sequentially, it is impossible to preprocess the dataset as required when training most deep loop closure detection models; 2) It is impossible to revisit previously observed environments. In the case where environments look drastically different from each other, sequential training can cause the network to forget knowledge learned from previous environments in favor of learning a new environment, which is known as the catastrophic forgetting.

#### IV. METHOD

##### A. Contrastive Learning for Loop Closure Detection

We follow the common visual place recognition pipeline [7] by learning an LCD model for generating global descriptors and using descriptor similarities to predict loop closure. Concretely, let  $\mathcal{I} = \bigcup_{i=1}^T \mathcal{I}^{(i)}$  be the collection of all images from all environments and  $f(\cdot; \theta) : \mathcal{I} \mapsto \mathbb{R}^D$  be the descriptor network parametrized by  $\theta$  that produces a global descriptor of length  $D$  for a given input image. Let  $I \in \mathcal{I}^{(t)}$  and  $\mathbf{D} \subset \mathcal{I}^{(t)}$  be the query and database from environment  $t$ , we retrieve the subset of  $\mathbf{D}$  with sufficiently high descriptor similarity:

$$\tilde{C}^{(t)}(I, \mathbf{D}) = \{I' \in \mathbf{D} : \text{sim}(f(I'), f(I)) \geq 1 - \epsilon\}. \quad (4)$$

where  $\epsilon \in (0, 1)$  is a constant and  $\text{sim}(\cdot, \cdot)$  is the cosine similarity. Let  $I_a, I_p, I_n \in \mathcal{I}^{(t)}$  be a triplet of images (namely, the anchor, the positive, and the negative) from the  $t$ -th environment, such that for the positive (loop-closing) pair,  $l^{(t)}(I_a, I_p) = 1$  and for the negative (irrelevant) pair,  $l^{(t)}(I_a, I_n) = 0$ . We calculate descriptor similarities  $s_{ap} = \text{sim}(f(I_a), f(I_p))$  and  $s_{an} = \text{sim}(f(I_a), f(I_n))$  and apply the triplet loss [49], which can be represented as

$$L_{\text{triplet}}^{(t)} = \max(s_{an} - s_{ap} + \delta, 0), \quad (5)$$

where  $\delta$  is a constant margin. Intuitively, this forces the network to predict similar descriptors for the positive pair  $(I_a, I_p)$  but distinct descriptors for the negative pair  $(I_a, I_n)$ . However, due to the sequential data access constraint, it is difficult to sample triplets from the data stream (3). We next demonstrate a triplet sampling technique for streaming data.

##### B. Buffered Triplet Sampling

In regular contrastive learning, the triplet is usually uniformly sampled from the set of all possible triplets of the current environment:  $(I_a, I_p, I_n) \sim \{(I'_a, I'_p, I'_n) \in \mathcal{I}^{(t)} : l^{(t)}(I'_a, I'_p) = 1, l^{(t)}(I'_a, I'_n) = 0\}$ . However, given constraints in Section III that the data items are only available sequentially, this scheme is not directly applicable. To resolve the issue, we maintain a similarity-aware memory buffer  $(\mathcal{M}^{(t)}, \mathbf{S}^{(t)})$  for environment  $t$  to temporarily store a fixed number of past images together with the ground-truth from  $l^{(t)}$ . Specifically, the memory  $\mathcal{M}^{(t)}$  is a first-in-first-out image queue of size  $M$  and the matrix  $\mathbf{S}^{(t)} \in \{0, 1\}^{M \times M}$  records the pairwise relationship for images in  $\mathcal{M}^{(t)}$  such that

$$S_{ij}^{(t)} = l^{(t)}(\mathcal{M}^{(t)}[i], \mathcal{M}^{(t)}[j]). \quad (6)$$

When a new image arrives, we replace the oldest image in  $\mathcal{M}^{(t)}$  with the new image and update  $\mathbf{S}^{(t)}$  according to (6).

To sample a triplet from  $\mathcal{M}^{(t)}$ , we first uniformly randomly select an anchor  $I_a = \mathcal{M}^{(t)}[a]$ . The positive  $I_p$  and negative  $I_n$  are then uniformly randomly drawn from the buffer such that  $S_{an} = 0$  and  $S_{ap} = 1$ .

##### C. Relational Memory Aware Synapses

It is commonly hypothesized in regularization-based life-long learning methods that catastrophic forgetting happens when learning of new tasks alters the network parameters that are important for previously learned tasks [11], [50]. To prevent such undesirable updates when learning the  $t$ -th task, MAS [13] assigns an importance weight  $\text{MAS}_{\Omega_i}^{(t)}$  to each parameter  $\theta_i$  and penalize its changes by the regularization loss. In this paper, we use a relational MAS (RMAS) loss:

$$L_{\text{RMAS}}^{(t)} = \sum_{i=1}^m \text{RMAS}_{\Omega_i}^{(t-1)} \left( \theta_i - \theta_i^{(t-1)} \right)^2, \quad (7)$$

where  $m$  is the number of network parameters and  $\theta_i^{(t-1)}$  is the parameter after learning tasks  $1, \dots, t-1$ .

In MAS [13],  $\text{MAS}_{\Omega_i}^{(t)}$  is estimated by the sensitivity of the network's output to the corresponding parameter:

$$\text{MAS}_{\Omega_i}^{(t)} = \mathbb{E}_{I \sim \mathcal{I}^{(t)}} \left( \frac{\partial \|f(I)\|_2}{\partial \theta_i} \right)^2, \quad (8)$$

where  $I$  is drawn from the image stream of the  $t$ -th environment and  $\|\cdot\|_2$  is the  $\ell_2$ -norm. Unlike in classification tasks, where the components of network output are tied to fixed classes, LCD pays less attention to the exact values of place descriptors but focuses more on their pairwise similarities.



Therefore, in RMAS, we instead penalize the changes to the pairwise similarity  $\text{sim}(f(I), f(I'))$  by setting

$$\text{RMAS}\Omega_i^{(t)} = \mathbb{E}_{I, I' \sim \mathcal{I}^{(t)}} \left( \frac{\partial \text{sim}(f(I), f(I'))}{\partial \theta_i} \right)^2. \quad (9)$$

Directly evaluating (9) is difficult under the lifelong learning setting since it requires the availability of all sample pairs from the current environment. Moreover, in an environment with  $N$  images, the derivative in (9) is calculated  $N(N-1)/2$  times. To make it computationally tractable, we approximate it by accumulating the squared gradient of the Gram matrix’s Frobenius norm from triplets sampled at each training step:

$$\text{RMAS}\Omega_i^{(t)} \approx \frac{1}{N_t} \sum_{k=1}^{N_t} \left( \frac{\partial \|\tilde{\mathbf{S}}_k^{(t)}\|_F}{\partial \theta_i} \right)^2, \quad (10)$$

where  $\|\cdot\|_F$  is the Frobenius norm and  $\tilde{\mathbf{S}}_k^{(t)} \in \mathbb{R}^{3 \times 3}$  is the Gram matrix at the  $k$ -th training step in environment  $t$ , which is formed by the output triplet  $f(I_a), f(I_p), f(I_n)$  such that  $\tilde{S}_{k,12} = \text{sim}(f(I_a), f(I_p))$ ,  $\tilde{S}_{k,13} = \text{sim}(f(I_a), f(I_n))$ , etc. After collecting importance weights  $\text{RMAS}\Omega_i^{(t-1)}$  in the  $\mathcal{E}^{(t-1)}$ , we use (7) to protect the important parameters in  $\mathcal{E}^{(t)}$ .

#### D. Relational Knowledge Distillation

It is known that knowledge distillation can be combined with parameter regularization to achieve less forgetting [51]. Therefore, we apply the knowledge distillation loss to alleviate forgetting by forcing the current model  $f(I, \theta)$  to retain the descriptor distances learned in environment  $1, \dots, t-1$ , which we call relational knowledge distillation (RKD):

$$L_{\text{RKD}}^{(t)} = \|\tilde{\mathbf{S}}^{(t)} - \tilde{\mathbf{S}}^{(t-1)}\|_F, \quad (11)$$

where  $\tilde{\mathbf{S}}^{(t)}$  is the triplet Gram matrix for the current training step defined in (10), and  $\tilde{\mathbf{S}}^{(t-1)}$  is its counterpart produced by  $f(I, \theta^{(t-1)})$ . Note that the input images  $I_a, I_p, I_n$  are drawn from the current environment, eliminating the need to preserve data from previous environments. This approach is similar to [30], where  $\tilde{\mathbf{S}}^{(t-2)}, \dots, \tilde{\mathbf{S}}^{(1)}$  are additionally estimated and used as targets in (11). However, we experimentally found that it is sufficient to only consider (11) in our setting.

#### E. Combined Loss for Lifelong Learning

We adopt a combined loss  $L^{(t)}$  for the  $t$ -th environment:

$$L^{(t)} = L_{\text{triplet}}^{(t)} + \lambda_1 L_{\text{RMAS}}^{(t)} + \lambda_2 L_{\text{RKD}}^{(t)}, \quad (12)$$

where  $\lambda_1, \lambda_2$  are hyperparameters. In the experiments, we show that although both  $L_{\text{RMAS}}^{(t)}$  and  $L_{\text{RKD}}^{(t)}$  alone is effective at alleviating forgetting and encouraging generalization, the combined loss yields a noticeably better result.

### V. EXPERIMENTS

#### A. Network Structure & Implementation Details

We adopt a pretrained VGG-19 as the feature extractor and use GeM [41] as the feature aggregator to produce a descriptor of dimension 1024. That is, after obtaining the highest-level feature map, we calculate the mean feature over

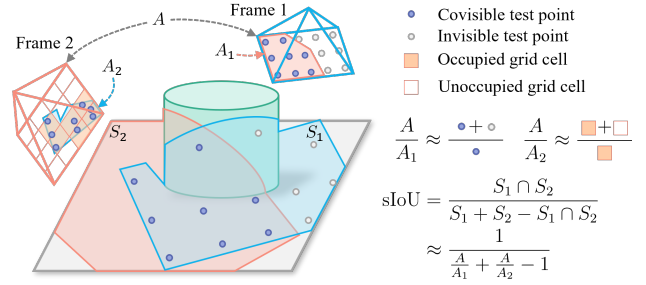


Fig. 2: We take the surface IoU to indicate a true loop closure. Specifically, we quantify the overlap between two camera frames by the IoU of surfaces ( $S_1$  and  $S_2$ ) captured by both cameras. To make it computationally tractable, we further estimate the area ratios on the screen:  $\frac{S_1}{S_1 \cap S_2} \approx \frac{A}{A_1}$  and  $\frac{S_2}{S_1 \cap S_2} \approx \frac{A}{A_2}$ , which is approximated by projecting a grid of test points from one camera to the other and counting the number of grid cells occupied by the covisible test points.

all pixels and transform it with a two-layer perceptron. We use the SGD optimizer with a learning rate of 0.002 and a momentum of 0.9. For each dataset described in Section V-B, we sequentially train the network with our method and the baselines in different environments and use the parameters obtained from environment  $t$  to initialize the network at environment  $t+1$ . The memory size  $M$  is fixed at 1000.

#### B. Datasets

We evaluate our method on one large-scale synthetic dataset, TartanAir [8] as well as two real-world datasets, Nordland [52], and RobotCar [53].

**Nordland** There are four seasonal environments in the Nordland dataset, namely, spring, summer, fall, and winter. We use the recommended train-test split and label the pairs with a maximum distance of 3 frames as loop closure.

**RobotCar** There are three environments based on the lighting condition, labeled sun, overcast, and night. For each environment, we select two sequences as the training and test set, respectively. Loop closure is defined as frames with distance less than 10m and yaw difference less than  $15^\circ$ .

**TartanAir** TartanAir is a large (about 3TB) and very challenging visual SLAM dataset consisting of binocular RGB-D video sequences together with additional per-frame information such as camera poses, optical flow, and semantic annotations. It features environments with various themes including urban, rural, natural, domestic, sci-fi, etc. We choose five scenes from the dataset and take 80% of the sequences from each scene for training and the rest for testing. Unlike Nordland or RobotCar, whose trajectories span a large space, TartanAir’s trajectories are more compact and convoluted.

In some of the sequences, we find that the Euclidean or timestamp distance is not a good indicator of loop closure since two frames taken from spatially close positions may look at different directions and vice versa. Therefore, we use “visual overlap” to define loop closure: Let  $A$  be the screen area and  $A_1, A_2$  be the area of covisible parts of the scene in

TABLE I: Performance comparison for lifelong loop closure detection. <sup>†</sup>

	TartanAir			Nordland			RobotCar		
	AP	BWT	FWT	AP	BWT	FWT	AP	BWT	FWT
Finetune	0.754±0.002	-0.009±0.006	0.730±0.001	0.615±0.014	-0.012±0.012	0.549±0.012	0.411±0.016	-0.066±0.007	0.462±0.011
EWC [26]	0.758±0.006	-0.005±0.003	0.728±0.004	0.614±0.020	-0.014±0.010	0.549±0.015	0.416±0.004	-0.054±0.017	0.461±0.013
SI [27]	0.753±0.003	-0.010±0.003	0.730±0.002	0.614±0.015	-0.010±0.012	0.549±0.012	0.407±0.013	-0.062±0.023	0.454±0.005
AirLoop <sup>w/o</sup> RMAS	0.757±0.001	-0.008±0.004	<u>0.733±0.002</u>	<b>0.632±0.020</b>	<u>0.008±0.009</u>	<b>0.549±0.024</b>	0.447±0.017	-0.041±0.027	0.472±0.015
AirLoop <sup>w/o</sup> RKD	0.759±0.005	-0.001±0.002	0.732±0.001	0.622±0.012	0.006±0.012	0.545±0.013	<u>0.456±0.006</u>	<b>-0.010±0.007</b>	<b>0.486±0.007</b>
AirLoop	<b>0.769±0.002</b>	<b>0.007±0.002</b>	<b>0.736±0.003</b>	<u>0.631±0.012</u>	<b>0.018±0.009</b>	<u>0.546±0.017</u>	<b>0.461±0.009</b>	<u>-0.013±0.011</u>	<u>0.485±0.013</u>
IFGIR*	0.753±0.003	-0.008±0.003	0.733±0.002	0.639±0.019	0.008±0.007	0.560±0.020	0.446±0.007	-0.030±0.007	0.476±0.009
Joint <sup>‡</sup>	0.772±0.003	-	-	0.650±0.023	-	-	0.485±0.011	-	-

<sup>†</sup>We highlight the best performance in each metric with **bold** and the second-best with underline. Each experiment is repeated 3 times. AP (average performance) is measured by recall @ 100% precision. Forward transfer (FWT) and backward transfer (BWT) are defined in (14).

\*IFGIR [30] requires a separate validation dataset for estimating previous outputs from the most recent teacher model, which cannot meet the requirements of lifelong learning, we instead save all historical teacher models during training. This produces a theoretical upper bound performance for IFGIR.

<sup>‡</sup>Joint training is expected to produce the theoretical upper-bound performance for lifelong learning, thus only average performance can be reported. The performance of AirLoop is close to this upper bound, indicating its effectiveness.

the two frames. We define the surface intersection-over-union (sIoU) in (13), as illustrated in Fig. 2.

$$\text{sIoU} = \frac{1}{A/A_1 + A/A_2 - 1}. \quad (13)$$

We take  $\text{sIoU} > 0.7$  as positive and  $\text{sIoU} < 0.1$  as negative during training and take  $\text{sIoU} > 0.5$  as positive during testing.

### C. Evaluation Metrics

Precision is paramount for LCD tasks since any incorrect matches may lead to fatal map degradation [54]. Therefore, we choose the recall rate at 100% precision as the metric of model performance. To better measure the interference between the learning of different environments, we evaluate the model performance on all environments, including the ones that haven't been trained on, after learning each environment. Therefore, for a dataset with  $T$  environments, we obtain a  $T \times T$  performance matrix  $\mathbf{R}$ , where  $R_{i,j}$  denotes the performance on environment  $j$  after learning environment  $i$ . We adopt the evaluation protocol (14) to summarize  $\mathbf{R}$  into three scalar metrics, which were introduced in [17].

$$\begin{aligned} \text{AP} &= (\sum_{i=1}^T \sum_{j=1}^i R_{i,j}) / (T(T+1)/2), \\ \text{BWT} &= (\sum_{i=2}^T \sum_{j=1}^{i-1} R_{i,j} - R_{j,j}) / (T(T-1)/2), \\ \text{FWT} &= (\sum_{i=1}^T \sum_{j=i+1}^T R_{i,j}) / (T(T-1)/2), \end{aligned} \quad (14)$$

where AP (average performance) is the overall performance on seen environments, BWT (backward transfer) accounts for the influence of future learning on knowledge learned from previous environments, and FWT (forward transfer) measures the generalization in unseen environments.

### D. Methods for Comparison

We compare the following methods:

1) *Finetune*: The network is finetuned on new environments only with the triplet loss  $L_{\text{triplet}}$ .

2) *EWC/SI*: Two generic regularization-based lifelong learning methods, elastic weight consolidation (EWC) [26] and synaptic intelligence [27].

3) *AirLoop*: Our method presented in Section IV.

4) *AirLoop<sup>w/o</sup> RMAS*: Our AirLoop network without the RMAS loss presented in Section IV-C.

5) *AirLoop<sup>w/o</sup> RKD*: Our AirLoop network without the RKD loss described in Section IV-D.

6) *IFGIR\**: The upper-bound of incremental fine-grained image retrieval (IFGIR) [30]. The original method requires a separate validation set, which is not available in the lifelong data setting. Instead, we implement its reported upper-bound of [30], which uses models learned from all previous environments to perform relational knowledge distillation.

7) *Joint*: Triplets can be sampled from any environment in arbitrary order. This gives the performance upper-bound.

### E. Performance

We report the overall performance in Table I. It can be seen that the Finetuned model exhibits a more negative BWT, which means that forgetting is problematic if lifelong learning techniques are not applied. In contrast, AirLoop is the only method that exhibits positive BWT on both TartanAir and Nordland, demonstrating its strong ability to not only retain but also extend previously learned knowledge.

In terms of AP / FWT, we only obtain very modest performance from generic regularization-based methods (EWC and SI) despite careful hyperparameter search. In comparison, AirLoop is able to outperform them by a noticeable margin and is advantageous than IFGIR\* on TartanAir and RobotCar. This shows the advantage of our methods at encouraging generalization. We notice that IFGIR\* is dominating in AP and FWT on Nordland. This is because the scene appearance in Nordland is quite similar for spring, summer, and fall environments, which allows the teacher models to remain informative and facilitates knowledge transfer. However, one shall not expect environments to be similar in all cases, especially in the setting of lifelong learning.

### F. Computational Efficiency

We list the running time of different operations taken during one training step in Table IIa. It can be observed that storing and sampling from the memory buffer only introduce a small overhead compared with the back-propagation. We further

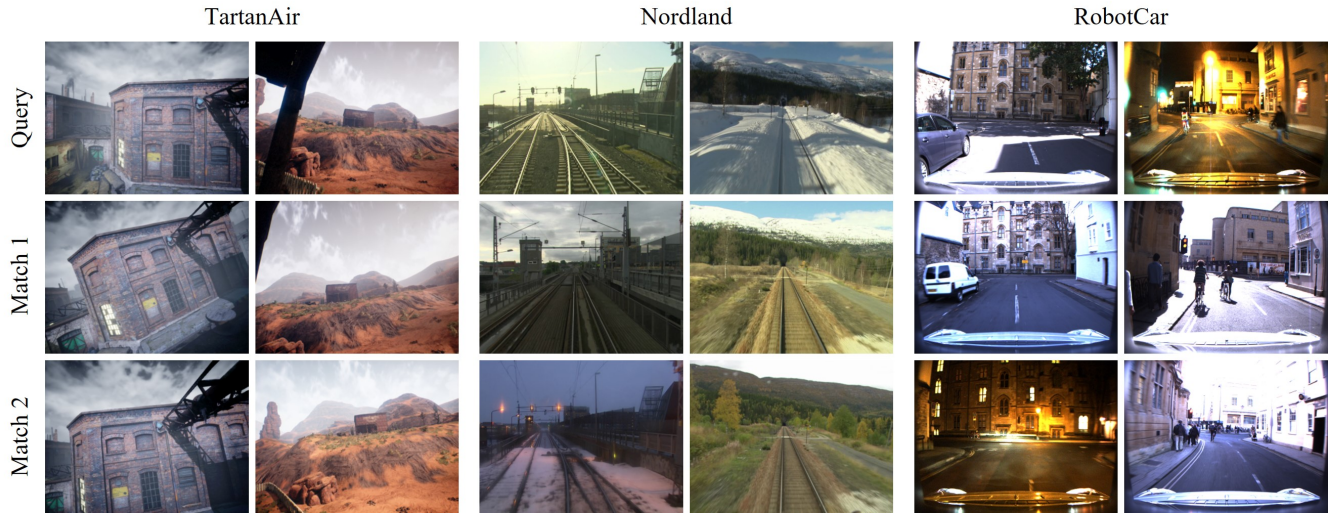


Fig. 3: Examples of loop closure detection after learning all environments on each dataset. Note that our model is trained incrementally with triplets from individual environments but is able to perform cross-environment loop closure detection.

TABLE II: Runtime Analysis.

(a) Runtime of steps		(b) Runtime of methods	
Operations	Time (ms)	Methods	Time (ms)
Memory store	66.5	IFGIR*	452.9
Memory sample	23.4	AirLoop <sup>w/o</sup> RKD	193.1
Evaluate $L_{\text{triplet}}$	17.8	AirLoop <sup>w/o</sup> RMAS	97.9
Back-propagation	185.5	AirLoop	292.3

compare the running time of the forward pass of different lifelong methods in Table IIb. Note that our method only requires 60% running time of IFGIR\*.

## VI. ABLATION STUDIES

### A. Memory Size

One major function of the memory buffer is to provide more choices of triplets so that the distribution of the sampled triplets can approach that of the whole dataset. Here we investigate the influence of memory size  $M$  on performance. We take RobotCar and Nordland as examples and present the final AP in Fig. 4. It can be seen that with a manageable

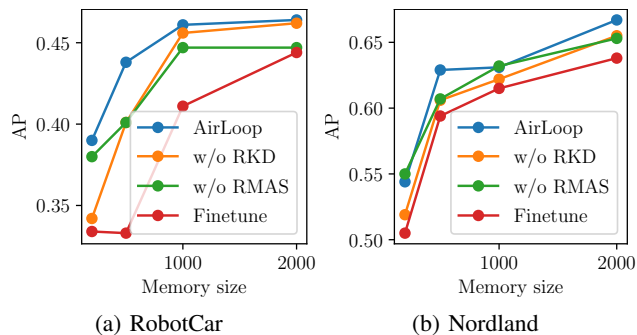


Fig. 4: Impact of memory buffer size on average performance (recall @ 100% precision) after learning all environments.

TABLE III: Comparison between relational and non-relational variant of MAS and KD.

	AP	BWT	FWT
Finetune	0.411 $\pm$ 0.016	-0.066 $\pm$ 0.007	0.462 $\pm$ 0.011
KD	0.414 $\pm$ 0.003	-0.058 $\pm$ 0.014	0.467 $\pm$ 0.014
<b>RKD</b>	<b>0.447 <math>\pm</math> 0.017</b>	<b>-0.041 <math>\pm</math> 0.027</b>	<b>0.472 <math>\pm</math> 0.015</b>
MAS	0.446 $\pm$ 0.010	-0.023 $\pm$ 0.012	0.482 $\pm$ 0.010
<b>RMAS</b>	<b>0.456 <math>\pm</math> 0.006</b>	<b>-0.010 <math>\pm</math> 0.007</b>	<b>0.486 <math>\pm</math> 0.007</b>

memory size of a few hundred to 1000, our proposed method is able to reach its peak performance.

### B. Relational Knowledge Preservation

We present the comparison between relational and non-relational variants of MAS and KD on RobotCar in Table III. It is observed that our two relational losses (RKD and RMAS) bring higher performance than non-relational losses (KD and MAS), which indicates the effectiveness of our method. Note that the non-relational losses tend to preserve the absolute values of the original descriptors, while our relational losses only retain the relative relationship between the descriptors. This allows our methods to focus on maintaining descriptor similarity, the property we care the most about.

## VII. CONCLUSIONS

We propose AirLoop, a method for incrementally training deep loop closure detection models. To enable triplet sampling, we implement a similarity-aware memory buffer to cache recently observed frames together with their pairwise similarity. We also formulate two lifelong relation learning losses, RMAS and RKD, for alleviating catastrophic forgetting in loop closure detection. Extensive experiments demonstrate the advantage of AirLoop in lifelong loop closure detection. Future work may consider more complicated backbone networks or incorporate memory replay methods.

## REFERENCES

- [1] X. Zhang, Y. Su, and X. Zhu, "Loop closure detection for visual slam systems using convolutional neural network," in *2017 23rd International Conference on Automation and Computing (ICAC)*. IEEE, 2017, pp. 1–6.
- [2] S. Arshad and G.-W. Kim, "Role of deep learning in loop closure detection for visual and lidar slam: A survey," *Sensors*, vol. 21, no. 4, p. 1243, 2021.
- [3] N. Dalal and B. Triggs, "Histograms of oriented gradients for human detection," in *2005 IEEE computer society conference on computer vision and pattern recognition (CVPR'05)*, vol. 1. Ieee, 2005, pp. 886–893.
- [4] D. G. Lowe, "Distinctive image features from scale-invariant keypoints," *International journal of computer vision*, vol. 60, no. 2, pp. 91–110, 2004.
- [5] H. Bay, A. Ess, T. Tuytelaars, and L. Van Gool, "Speeded-up robust features (surf)," *Computer vision and image understanding*, vol. 110, no. 3, pp. 346–359, 2008.
- [6] D. Nister and H. Stewenius, "Scalable recognition with a vocabulary tree," in *2006 IEEE Computer Society Conference on Computer Vision and Pattern Recognition (CVPR'06)*, vol. 2. Ieee, 2006, pp. 2161–2168.
- [7] C. Masone and B. Caputo, "A survey on deep visual place recognition," *IEEE Access*, vol. 9, pp. 19 516–19 547, 2021.
- [8] W. Wang, D. Zhu, X. Wang, Y. Hu, Y. Qiu, C. Wang, Y. Hu, A. Kapoor, and S. Scherer, "Tartanair: A dataset to push the limits of visual slam," *2020 IEEE/RSJ International Conference on Intelligent Robots and Systems (IROS)*, 2020.
- [9] C. Wang, Y. Qiu, W. Wang, Y. Hu, S. Kim, and S. Scherer, "Unsupervised online learning for robotic interestingness with visual memory," *IEEE Transactions on Robotics*, 2021.
- [10] E. Garcia-Fidalgo and A. Ortiz, "ibow-lcd: An appearance-based loop-closure detection approach using incremental bags of binary words," *IEEE Robotics and Automation Letters*, vol. 3, no. 4, pp. 3051–3057, 2018.
- [11] T. Lesort, V. Lomonaco, A. Stoian, D. Maltoni, D. Filliat, and N. Diaz-Rodriguez, "Continual learning for robotics," *arXiv preprint arXiv:1907.00182*, pp. 1–34, 2019.
- [12] G. I. Parisi, R. Kemker, J. L. Part, C. Kanan, and S. Wermter, "Continual lifelong learning with neural networks: A review," *Neural Networks*, vol. 113, pp. 54–71, 2019.
- [13] R. Aljundi, F. Babiloni, M. Elhoseiny, M. Rohrbach, and T. Tuytelaars, "Memory aware synapses: Learning what (not) to forget," in *Proceedings of the European Conference on Computer Vision (ECCV)*, 2018, pp. 139–154.
- [14] S. Hou, X. Pan, C. C. Loy, Z. Wang, and D. Lin, "Lifelong learning via progressive distillation and retrospection," in *Proceedings of the European Conference on Computer Vision (ECCV)*, 2018, pp. 437–452.
- [15] M. Delange, R. Aljundi, M. Masana, S. Parisot, X. Jia, A. Leonardis, G. Slabaugh, and T. Tuytelaars, "A continual learning survey: Defying forgetting in classification tasks," *IEEE Transactions on Pattern Analysis and Machine Intelligence*, 2021.
- [16] S.-A. Rebuffi, A. Kolesnikov, G. Sperl, and C. H. Lampert, "icarl: Incremental classifier and representation learning," in *Proceedings of the IEEE conference on Computer Vision and Pattern Recognition*, 2017, pp. 2001–2010.
- [17] D. Lopez-Paz and M. Ranzato, "Gradient episodic memory for continual learning," *Advances in neural information processing systems*, vol. 30, pp. 6467–6476, 2017.
- [18] D. Rolnick, A. Ahuja, J. Schwarz, T. P. Lillicrap, and G. Wayne, "Experience replay for continual learning," *arXiv preprint arXiv:1811.11682*, 2018.
- [19] D. Isele and A. Cosgun, "Selective experience replay for lifelong learning," in *Proceedings of the AAAI Conference on Artificial Intelligence*, vol. 32, no. 1, 2018.
- [20] H. Shin, J. K. Lee, J. Kim, and J. Kim, "Continual learning with deep generative replay," *arXiv preprint arXiv:1705.08690*, 2017.
- [21] C. Atkinson, B. McCane, L. Szymanski, and A. Robins, "Pseudo-recursion: Solving the catastrophic forgetting problem in deep neural networks. arxiv 2018," *arXiv preprint arXiv:1802.03875*, vol. 2, 2018.
- [22] Z. Li and D. Hoiem, "Learning without forgetting," *IEEE transactions on pattern analysis and machine intelligence*, vol. 40, no. 12, pp. 2935–2947, 2017.
- [23] A. Rannen, R. Aljundi, M. B. Blaschko, and T. Tuytelaars, "Encoder based lifelong learning," in *Proceedings of the IEEE International Conference on Computer Vision*, 2017, pp. 1320–1328.
- [24] A. Mallya and S. Lazebnik, "Packnet: Adding multiple tasks to a single network by iterative pruning," in *Proceedings of the IEEE conference on Computer Vision and Pattern Recognition*, 2018, pp. 7765–7773.
- [25] A. Mallya, D. Davis, and S. Lazebnik, "Piggyback: Adapting a single network to multiple tasks by learning to mask weights," in *Proceedings of the European Conference on Computer Vision (ECCV)*, 2018, pp. 67–82.
- [26] J. Kirkpatrick, R. Pascanu, N. Rabinowitz, J. Veness, G. Desjardins, A. A. Rusu, K. Milan, J. Quan, T. Ramalho, A. Grabska-Barwinska, et al., "Overcoming catastrophic forgetting in neural networks," *Proceedings of the national academy of sciences*, vol. 114, no. 13, pp. 3521–3526, 2017.
- [27] F. Zenke, B. Poole, and S. Ganguli, "Continual learning through synaptic intelligence," in *International Conference on Machine Learning*. PMLR, 2017, pp. 3987–3995.
- [28] A. Chaudhry, P. K. Dokania, T. Ajanthan, and P. H. Torr, "Riemannian walk for incremental learning: Understanding forgetting and intransigence," in *Proceedings of the European Conference on Computer Vision (ECCV)*, 2018, pp. 532–547.
- [29] W. Chen, Y. Liu, W. Wang, T. Tuytelaars, E. M. Bakker, and M. Lew, "On the exploration of incremental learning for fine-grained image retrieval," *arXiv preprint arXiv:2010.08020*, 2020.
- [30] W. Chen, Y. Liu, N. Pu, W. Wang, L. Liu, and M. S. Lew, "Feature estimations based correlation distillation for incremental image retrieval," *IEEE Transactions on Multimedia*, 2021.
- [31] C. Wang, Y. Qiu, and S. Scherer, "Lifelong graph learning," *arXiv preprint arXiv:2009.00647*, 2020.
- [32] D. Gálvez-López and J. D. Tardos, "Bags of binary words for fast place recognition in image sequences," *IEEE Transactions on Robotics*, vol. 28, no. 5, pp. 1188–1197, 2012.
- [33] M. Cummins and P. Newman, "Fab-map: Probabilistic localization and mapping in the space of appearance," *The International Journal of Robotics Research*, vol. 27, no. 6, pp. 647–665, 2008.
- [34] R. Paul and P. Newman, "Fab-map 3d: Topological mapping with spatial and visual appearance," in *2010 IEEE international conference on robotics and automation*. IEEE, 2010, pp. 2649–2656.
- [35] S. Khan and D. Wollherr, "Ibuid: Incremental bag of binary words for appearance based loop closure detection," in *2015 IEEE International Conference on Robotics and Automation (ICRA)*. IEEE, 2015, pp. 5441–5447.
- [36] K. Simonyan and A. Zisserman, "Very deep convolutional networks for large-scale image recognition," *arXiv preprint arXiv:1409.1556*, 2014.
- [37] K. He, X. Zhang, S. Ren, and J. Sun, "Deep residual learning for image recognition," in *Proceedings of the IEEE conference on computer vision and pattern recognition*, 2016, pp. 770–778.
- [38] C. Szegedy, V. Vanhoucke, S. Ioffe, J. Shlens, and Z. Wojna, "Rethinking the inception architecture for computer vision," in *Proceedings of the IEEE conference on computer vision and pattern recognition*, 2016, pp. 2818–2826.
- [39] R. Arandjelovic, P. Gronat, A. Torii, T. Pajdla, and J. Sivic, "Netvlad: Cnn architecture for weakly supervised place recognition," in *Proceedings of the IEEE conference on computer vision and pattern recognition*, 2016, pp. 5297–5307.
- [40] A. Gordo, J. Almazan, J. Revaud, and D. Larlus, "End-to-end learning of deep visual representations for image retrieval," *International Journal of Computer Vision*, vol. 124, no. 2, pp. 237–254, 2017.
- [41] F. Radenović, G. Toliás, and O. Chum, "Fine-tuning cnn image retrieval with no human annotation," *IEEE transactions on pattern analysis and machine intelligence*, vol. 41, no. 7, pp. 1655–1668, 2018.
- [42] Z. Zhang, T. Sattler, and D. Scaramuzza, "Reference pose generation for long-term visual localization via learned features and view synthesis," *International Journal of Computer Vision*, vol. 129, no. 4, pp. 821–844, 2021.
- [43] F. Han, H. Wang, and H. Zhang, "Learning integrated holism-landmark representations for long-term loop closure detection," in *Thirty-Second AAAI Conference on Artificial Intelligence*, 2018.
- [44] A. Khaliq, S. Ehsan, Z. Chen, M. Milford, and K. McDonald-Maier, "A holistic visual place recognition approach using lightweight cnns for significant viewpoint and appearance changes," *IEEE transactions on robotics*, vol. 36, no. 2, pp. 561–569, 2019.



- [45] Z. Chen, L. Liu, I. Sa, Z. Ge, and M. Chli, "Learning context flexible attention model for long-term visual place recognition," *IEEE Robotics and Automation Letters*, vol. 3, no. 4, pp. 4015–4022, 2018.
- [46] C. Linegar, W. Churchill, and P. Newman, "Work smart, not hard: Recalling relevant experiences for vast-scale but time-constrained localisation," in *2015 IEEE International Conference on Robotics and Automation (ICRA)*. IEEE, 2015, pp. 90–97.
- [47] P. Neubert, S. Schubert, and P. Protzel, "A neurologically inspired sequence processing model for mobile robot place recognition," *IEEE Robotics and Automation Letters*, vol. 4, no. 4, pp. 3200–3207, 2019.
- [48] S. An, H. Zhu, D. Wei, and K. A. Tsintotas, "Fast and incremental loop closure detection with deep features and proximity graphs," *arXiv preprint arXiv:2010.11703*, 2020.
- [49] F. Schroff, D. Kalenichenko, and J. Philbin, "Facenet: A unified embedding for face recognition and clustering," in *Proceedings of the IEEE conference on computer vision and pattern recognition*, 2015, pp. 815–823.
- [50] M. Masana, X. Liu, B. Twardowski, M. Menta, A. D. Bagdanov, and J. van de Weijer, "Class-incremental learning: survey and performance evaluation," *arXiv preprint arXiv:2010.15277*, 2020.
- [51] Y. Peng, L. Yuxuan, and L. Ming, "In defense of knowledge distillation for task incremental learning and its application in 3d object detection," *IEEE Robotics and Automation Letters*, vol. 6, no. 2, pp. 2012–2019, 2021.
- [52] D. Olid, J. M. Fàcil, and J. Civera, "Single-view place recognition under seasonal changes," *arXiv preprint arXiv:1808.06516*, 2018.
- [53] W. Maddern, G. Pascoe, C. Linegar, and P. Newman, "1 Year, 1000km: The Oxford RobotCar Dataset," *The International Journal of Robotics Research (IJRR)*, vol. 36, no. 1, pp. 3–15, 2017.
- [54] S. Garg, T. Fischer, and M. Milford, "Where is your place, visual place recognition?" *arXiv preprint arXiv:2103.06443*, 2021.